

Mechanism and Product Distribution of the O₃-Initiated Degradation of (*E*)-2-Heptenal, (*E*)-2-Octenal and (*E*)-2-Nonenal

Elizabeth Gaona Colmán^a, María B. Blanco^{a*}, Ian Barnes^b, Peter Wiesen^b and Mariano A. Teruel^{a*}

^a Instituto de Investigaciones en Físicoquímica de Córdoba (I.N.F.I.Q.C.), Facultad de Ciencias Químicas, Universidad Nacional de Córdoba. Ciudad Universitaria, 5000 Córdoba, Argentina.

^b Bergische Universität Wuppertal, Fakultät für Mathematik und Naturwissenschaften, Institut für Atmosphären und Umweltforschung, Gauss Strasse 20, 42119 Wuppertal, Germany.

*Corresponding authors: mteruel@fcq.unc.edu.ar.
mblanco@fcq.unc.edu.ar.

Abstract

The O₃-molecule initiated degradation of three 2-alkenals (*E*)-2-heptenal, (*E*)-2-octenal and (*E*)-2-nonenal has been investigated in a 1080 L quartz-glass environmental chamber at 298 ± 2 K and atmospheric pressure of synthetic air using *in situ* FTIR spectroscopy to monitor the reactants and products. The molar yields of the primary products formed were glyoxal (49 ± 4) % and pentanal (34 ± 3) % from the reaction of (*E*)-2-heptenal with O₃, glyoxal (41 ± 3) % and hexanal (39 ± 3) % from the reaction of (*E*)-2-octenal with O₃ and glyoxal (45 ± 3) % and heptanal (46 ± 3) % from the reaction of (*E*)-2-nonenal with O₃. The residual bands in the infrared product spectra for each of the studied reactions are attributed to 2-oxoaldehyde compounds. Based on the observed products, a general mechanism for the ozonolysis reaction of long chain unsaturated aldehydes is proposed and the results are compared with the available literature data.

Introduction

The C7-C9 2-alkenals (*E*)-2-heptenal, (*E*)-2-octenal and (*E*)-2-nonenal are volatile organic compounds present in cranberries,^{1,2} *Citrullus lanatus*,³ and raw potatoes.⁴ (*E*)-2-Nonenal has been detected as a volatile organic constituent of *Cucumis sativus* L.^{5,6} and apples.⁷ The emissions of these compounds are attributed to lipid oxidation in the vegetal membrane.⁸⁻¹⁰ Biodiesels also emit aldehydes, Cahill and Okamoto¹¹ and do N. Batista et al.¹² have reported among other aldehydes the emission of 2-heptenal from the combustion of soybean- and animal-based biodiesel. Additionally, oils at frying temperatures emit several aldehydes among them (*E*)-2-alkenal type aldehydes with C3-C11 carbon chains and also toxic oxygenated (*E*)-2-alkenal type aldehydes.¹³

38 Unsaturated aldehydes once emitted to the atmosphere will be subject to degradation by photolysis
39 and reaction with OH radicals during day and by reaction with NO₃ radicals during the late evening
40 and night. Reaction of unsaturated aldehydes with O₃ molecules is possible both day and night but
41 will only play a significant role in polluted areas with elevated ozone concentrations. Recent studies
42 have shown that the gas-phase and aqueous-phase oxidation of these compounds can form
43 secondary organic aerosols (SOA) and that they are precursors for polar organosulphates which
44 have been found in ambient aerosol.¹⁴⁻¹⁶

45 We have previously reported a kinetic study on the reaction of O₃ with (*E*)-2-heptenal, (*E*)-2-octenal
46 and (*E*)-2-nonenal at 298 K using the relative rate method, the obtained k_{O_3} in units of $\times 10^{18}$
47 ($\text{cm}^3\text{molecule}^{-1}\text{s}^{-1}$) were: (2.47 ± 0.73) for (*E*)-2-heptenal, (2.37 ± 0.68) for (*E*)-2-octenal and ($2.05 \pm$
48 0.20) for (*E*)-2-nonenal.¹⁷ These rate coefficients showed that for the studied long-chain aldehydes
49 increasing the alkyl chain length has a virtually negligible influence on the measured rate
50 coefficients, i.e. above C3 the electron-donating effect of the alkyl chain has no further effect on the
51 reactivity of the double bond toward O₃ addition. Kinetic studies for reaction of these aldehydes
52 with other atmospheric oxidants have been reported. A room temperature rate coefficient for the
53 reaction of OH radicals with (*E*)-2-heptenal has been reported by Albaladejo et al.¹⁸ and Davis et
54 al.¹⁹ have investigated the temperature dependence of the reaction over the range 244 – 374 K. Gao
55 et al.²⁰ have determined the rate coefficients for the reactions of OH radicals with (*E*)-2-octenal and
56 (*E*)-2-nonenal at 298K. A room temperature rate coefficient for the reaction of (*E*)-2-heptenal with
57 NO₃ radicals has been obtained by Zhao et al.²¹ Kerdouci et al.²² have reported a value for the same
58 reaction at 204 K in addition to a rate coefficient for the reaction of (*E*)-2-octenal with NO₃ radicals.
59 Finally, Rodríguez et al.²³ have measured the rate coefficient for the reaction of Cl atoms with (*E*)-
60 2-heptenal at room temperature.

61 There have been a number of previous product studies on the reaction of O₃ with unsaturated
62 aldehydes, most of them, however, on short-chain aldehydes (<C₆). Grosjean et al.²⁴ have studied
63 the products resulting from the ozonolysis of the C3 2-alkenal acrolein (CH₂=CHC(O)H) at
64 temperatures between 12-17°C, Grosjean and Grosjean²⁵ have investigated the products from the
65 ozonolysis of the C4 2-alkenal crotonaldehyde (CH₃CH=CHC(O)H) at room temperature and
66 Grosjean et al.²⁶ the products resulting from the reaction of O₃ with the C6 2-alkenal *trans*-2-
67 hexenal at ambient temperature. More recently, Uchida et al.²⁷ have studied the products produced
68 in the ozonolysis of the C6 3-alkenal (*Z*)-3-hexenal under atmospheric conditions. To our
69 knowledge, there are no previous products studies for the reactions of OH radicals with the C7-C9
70 2-alkenals under study in this work, however, Kerdouci et al.²² have reported product analyses for
71 the reactions of NO₃ radicals with (*E*)-2-hexenal, (*E*)-2-heptenal and (*E*)-2-octenal where they

72 observed that unsaturated peroxyxynitrate type compounds were the main products formed via H-atom
73 abstraction by NO_3 from the aldehyde entity and subsequent consecutive additions of O_2 and NO_2 to
74 the resulting $\text{CH}_3(\text{CH}_2)_n\text{CH}=\text{CHC}(=\text{O})$ radicals ($n = 2, 3$ or 4).

75 The primary aim of the present work is to identify and quantify the gas-phase products produced in
76 the room temperature ozonolysis of the long-chain C7-C9 2-alkenals (*E*)-2-heptenal, (*E*)-2-octenal
77 and (*E*)-2-nonenal. Identification of the primary reaction products generated in the ozonolysis of the
78 2-alkenals will provide information on the effect of the aldehyde functionality on the fragmentation
79 of the primary ozonide compared to that observed for alkyl substituted alkenes. The secondary aim
80 of the study is to postulate mechanisms for the reactions leading to the observed products and to
81 evaluate potential atmospheric implications of the reactions. To the best of our knowledge, this
82 work represents the first report of products and product yields for the ozonolysis of the long-chain
83 aldehydes (*E*)-2-heptenal, (*E*)-2-octenal and (*E*)-2-nonenal.

84

85 **Experimental set up**

86

87 A 1080 L reaction chamber was used to perform the experiments at (298 ± 2) K in 750 Torr of
88 synthetic air. The chamber consists of two cylindrical quartz glass vessels, each 3 m in length and
89 45 cm inner diameter, joined in the middle with both open ends closed by aluminium flanges. The
90 reactants and the bath gases were introduced through ports located on the metal flanges. To ensure
91 homogeneous mixing of the reactants three fans with Teflon blades are mounted inside the
92 chamber. The reaction chamber can be evacuated to $<10^{-3}$ Torr by a pumping system consisting of a
93 turbomolecular pump backed by a double stage rotary fore pump. White-type mirrors mounted
94 internally in the chamber are coupled via an external optical transfer system to a Thermo Nicolet
95 Nexus FTIR spectrometer. The “White” mirror system in the chamber was operated with the total
96 optical absorption path length set to 484.7 m. The spectrometer is equipped with a liquid nitrogen
97 cooled mercury-cadmium-telluride (MCT) detector. This setup enables “*in situ*” monitoring of the
98 reactants and products in the infrared range $4000\text{-}700\text{ cm}^{-1}$. Infrared spectra were recorded with a
99 spectral resolution of 1 cm^{-1} .

100 For the experiments of the ozonolysis of (*E*)-2-heptenal, 80 interferograms were co-added per
101 spectrum and 20 such spectra were recorded per experiment, for the ozonolysis of (*E*)-2-octenal 75
102 interferograms were co-added per spectrum and 22 such spectra were recorded per experiment and
103 for the ozonolysis of (*E*)-2-nonenal 100 interferograms were co-added per spectrum and 25 such
104 spectra were recorded per experiment. The reactor is described in greater details in Barnes et al.^{28,29}
105 Ozone was produced by flowing O_2 through an electrical discharge and was added continuously to

106 the chamber containing the aldehyde homogeneously mixed in synthetic air. The O₃ concentration
107 introduced into the chamber was up to a maximum of 7 ppmV. The experiments were performed in
108 the absence of an OH radical scavenger since addition of very large concentrations of scavengers
109 such as CO or cyclohexane would have been necessary to scavenge the OH in the reaction systems
110 and such large concentrations would have made an FTIR analysis of the system impossible. The
111 consequences of the non-use of an OH radical scavenger in the experiments for the results are
112 discussed in detail further in the Results and Discussion section. Two experiments were performed
113 for each of the studied reactions.

114 Reaction products were quantified by comparison with reference spectra contained in the IR
115 spectral database of the laboratory in Wuppertal. Pentanal and hexanal were quantified using
116 absorption cross sections from the database of the laboratory in Wuppertal while glyoxal and
117 heptanal were quantified using cross section values reported by Volkamer et al.³⁰ and Beaver et
118 al.,³¹ respectively. All three unsaturated aldehydes were monitored in the infrared absorption region
119 2700-3000 cm⁻¹. Identified products were monitored at the following infrared absorption regions (in
120 cm⁻¹): glyoxal, 2748-2910; pentanal, 2650-3000; hexanal, 2600-3000; heptanal, 2650-3000. The
121 initial concentrations of the unsaturated aldehydes in ppm (1 ppmV = 2.46 × 10¹³ molecule cm⁻³ at
122 298 K) were (*E*)-2-heptenal 0.87-0.88; (*E*)-2-octenal 0.77-0.83 and (*E*)-2-nonenal 0.64-0.66.

123 The chemicals used in the experiments had the following purities as given by the manufacturer and
124 were used as supplied: synthetic air (Air Liquide, 99.999%), (*E*)-2-heptenal (Aldrich 97%), (*E*)-2-
125 octenal (Aldrich, ≥95%) and (*E*)-2-nonenal (Aldrich, 97%)

126

127 **Results and Discussion**

128

129 Figure 1, panel A, shows the infrared spectrum of a (*E*)-2-heptenal/O₃/air gas mixture after reaction
130 and subtraction of residual (*E*)-2-heptenal. Reference spectra of glyoxal and pentanal are shown in
131 panels B and C, and panel D shows the residual product spectrum obtained after subtraction of
132 features due to the reference spectra from the spectrum in panel A. Similarly, Figure S1 (see
133 Supplementary Information, SI), panel A, shows the infrared spectrum of a (*E*)-2-octenal/O₃/air gas
134 mixture after reaction and subtraction of residual (*E*)-2-octenal (Panel A). Reference spectra of
135 glyoxal and hexanal are shown in panels B and C, and panel D shows the residual product spectrum
136 obtained after subtraction of features due to the reference spectra from the spectrum in panel A.
137 Figure S2 shows the same infrared spectral information obtained from experiments performed on a
138 (*E*)-2-nonenal/O₃/air gas mixture, however, in this case panel C shows a reference spectrum of
139 heptanal.

140 Formation of pentanal, hexanal and heptanal has been positively identified in the ozonolysis of (*E*)-
141 2-heptenal, (*E*)-2-octenal and (*E*)-2-nonenal, respectively. Glyoxal was identified as product in the
142 ozonolysis of all three unsaturated aldehydes. Concentration–time profiles of (*E*)-2-heptenal, (*E*)-2-
143 octenal and (*E*)-2-nonenal and the identified products are presented in Figures 2, S3 and S4,
144 respectively. Plots of the concentrations of the products as a function of consumed 2-alkenal are
145 shown in Figures 3, S5 and S6 for (*E*)-2-heptenal, (*E*)-2-octenal and (*E*)-2-nonenal, respectively.
146 Reasonably good linear correlations were observed in all cases. The molar product yields obtained
147 from linear least-squares analyses of the plots in Figures 3, S5 and S6 are listed in Table 1. The
148 errors given in Table 1 are the 2σ standard deviations from the analyses of the plots.

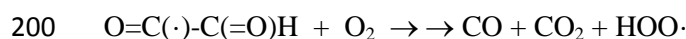
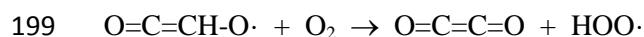
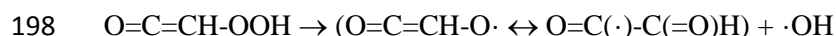
149 Ozonolysis reactions of unsaturated organics are initiated by addition of the O_3 molecule to the
150 double bond of the compound to form a 1,2,3-trioxolane primary ozonide. This primary ozonide is
151 energy rich and rapidly decomposes by cleavage of a C-C and an O-O bond to form a primary
152 carbonyl and an initially vibrationally excited biradical known as a Criegee Intermediate (CI). The
153 excited CI can unimolecularly decompose ejecting an $O(^3P)$ atom, isomerize to form a hydroperoxide,
154 rearrange to form an ester or acid or can be collisionally stabilized with the bath gas molecules.^{32,33}
155 The so-called hydroperoxide channel is known to form OH radicals to varying degrees through
156 decomposition of the hydroperoxide.³⁴⁻³⁶

157 A very simplified general mechanism for the reaction of O_3 with (*E*)-2-heptenal, (*E*)-2-octenal and
158 (*E*)-2-nonenal, not showing all possible reaction channels, is shown in Figure 4. The O_3 molecule
159 reacts with the 2-alkenals by addition to the double bond to form a primary ozonide, which
160 decomposes through channels A and B indicated in Figure 4. Decomposition of the ozonide through
161 channel A forms glyoxal $HC(O)C(O)H$ and $CH_3(CH_2)_nC\cdot HOO\cdot$ Criegee biradical where “n”
162 indicates the number of $-CH_2-$ groups, i.e. 3, 4 and 5 for (*E*)-2-heptenal, (*E*)-2-octenal and (*E*)-2-
163 nonenal, respectively. The vibrationally excited biradicals formed through channel A can
164 potentially react via the hydroperoxide channel. Decomposition of the hydroperoxide can produce
165 OH radicals and further reactions of the organic radical co-product can lead to the formation of a 2-
166 oxoaldehyde and a hydroperoxide radical as shown in Figure 4. Due to the lack of reference spectra
167 we are currently not able to unambiguously confirm whether or not the 2-oxoaldehyde formation
168 channel is operative. The alkoxy radical $(CH_3(CH_2)_mCH(O\cdot)CH(O))$ can also isomerize as it is
169 shown in Figure 4. We proposed the 1,5 hydrogen shift of the alkoxy radical when $m=2$ (from the
170 ozonolysis of (*E*)-2-heptenal). The isomerization and subsequent reaction with O_2 and peroxy
171 radical can lead to other 1,5 hydrogen shift of the new alkoxy radical to finally form a
172 hydroxydicarbonyl compound through reaction with O_2 . On the other hand, decomposition of the
173 primary ozonide through channel B forms the $HC(O)C\cdot HOO\cdot$ Criegee biradical and the

174 corresponding saturated aldehydes $\text{CH}_3(\text{CH}_2)_n\text{C}(\text{O})\text{H}$ ($n = 3, 4, \text{ or } 5$) which in the case of the
175 ozonolysis of (*E*)-2-heptenal, (*E*)-2-octenal and (*E*)-2-nonenal will be pentanal, hexanal and
176 heptanal, respectively.

177 Under our experimental conditions the ozonolysis of (*E*)-2-heptenal forms glyoxal and pentanal as
178 primary products with molar yields of $(49 \pm 4) \%$ and $(34 \pm 3) \%$, respectively. In the case of (*E*)-2-
179 octenal the primary products are glyoxal and hexanal with yields of $(41 \pm 3) \%$ and $(39 \pm 3) \%$,
180 respectively, and in the case of (*E*)-2-nonenal glyoxal and heptanal with yields of $(45 \pm 3) \%$ and
181 $(46 \pm 3) \%$, respectively. As mentioned previously in the Introduction section, the ozonolysis
182 products of the three 2-alkenals studied here have not been previously reported in the literature;
183 therefore, a direct comparison with other studies for the same 2-alkenals is not possible.

184 As already stated a number of times the ozonolysis of alkenes is known to produce OH radicals³⁶
185 which can influence the yields of the primary carbonyls measured in the ozonolysis of the 2-
186 alkenals studied here. The OH radical yields for the ozonolysis of a large number of alkenes have
187 been reported in the literature,³⁶ however, none have been reported to date for 2-alkenals under
188 study. Rickard et al.³⁷ have developed a structure activity relationship (SAR) to rationalize the OH
189 yields in ozone-alkene reactions as a function of the alkene structure, however, unfortunately this
190 SAR can not be applied to estimate OH yields for 2-alkenals. The Criegee biradicals formed in the
191 ozonolysis of the unsaturated aldehydes will have the structures $\text{CH}_3(\text{CH}_2)_n\text{C}\cdot\text{HOO}\cdot$ ($n = 3, 4 \text{ or } 5$)
192 and $\text{HC}(\text{=O})\text{C}\cdot\text{HOO}\cdot$ and can potentially form the hydroperoxides $\text{CH}_3(\text{CH}_2)_n\text{CH}=\text{CHOOH}$ ($n = 2,$
193 $3, 4$) and $\text{O}=\text{C}=\text{CH}-\text{OOH}$, respectively. It is known from studies on the ozonolysis of alkenes that
194 decomposition of $\text{CH}_3(\text{CH}_2)_n\text{CH}=\text{CHOOH}$ hydroperoxides will undoubtedly produce OH radicals
195 to some degree,³⁶ however, nothing is currently known about the formation and fate of the
196 $\text{O}=\text{C}=\text{CH}-\text{OOH}$ hydroperoxide. If $\text{O}=\text{C}=\text{CH}-\text{OOH}$ is formed, on decomposition it could form OH
197 radicals and ethylenedione ($\text{O}=\text{C}=\text{C}=\text{O}$) and/or CO/CO₂:

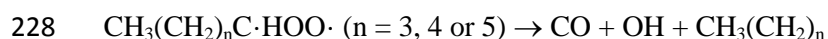


201

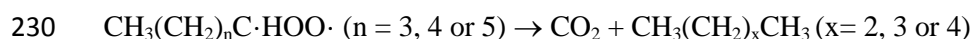
202 Ethylenedione has only recently been detected spectroscopically³⁸ and is known to be intrinsically
203 short-lived and to dissociate to give two ground-state CO molecules. If formed, and long enough
204 lived, it would absorb in the infrared region between the CO and CO₂ absorptions as is observed for

205 carbon suboxide (O=C=C=C=O).³⁹ In the infrared region from 2000 to 2400 cm⁻¹, only absorptions
206 due to CO and CO₂ are visible in the product spectra and there is nothing to indicate the
207 intermediary formation of a compound such as ethylenedione. Also the amount of CO that was in
208 the reaction system initially did not change during the course of the ozonolysis. Unfortunately, it is
209 not possible to say what the trend is in CO₂ since the signal in the CO₂ absorption region is
210 saturated due to CO₂ in the transfer optics housing between the chamber and FTIR spectrometer.
211 However, the infrared and CO concentration observations support that the O=C=CH-OOH
212 hydroperoxide channel and thus OH radical formation is probably not occurring for the
213 HC(=O)C·HOO· Criegee biradical. Possible other reactions of the excited HC(=O)C·HOO·
214 biradical include i) ejection of an O atom through *the O-atom channel* to form glyoxal, ii)
215 isomerization via *the "hot" acid channel* with formation of glyoxylic acid (HC(=O)C(=O)OH) and
216 iii) stabilization of the excited biradical. The product spectra of the three alkenals were compared
217 with an IR spectrum of glyoxylic acid and we do not observed the formation of this acid (see
218 Figure S7), therefore, we assumed that ejection of an O-atom to form glyoxal and collisional
219 stabilization of the biradical are the main fates of the excited HC(=O)C·HOO· biradical. The
220 stabilized HC(=O)C·HOO· biradical is also quite likely under our experimental conditions to react
221 further to form glyoxal. This observation has consequences for the interpretation of the preferred
222 fragmentation channel of the primary ozonide and is discussed further below. Additionally, Uchida
223 et al.²⁷ in their study of the ozonolysis of (*Z*)-3-hexenal proposed that the alkyl chain biradical can
224 decompose through two pathway. Based on their work, the alkyl substituted biradical of the
225 ozonolysis reaction under study CH₃(CH₂)_nC·HOO· (n = 3, 4 or 5) can undergo the following
226 decomposition pathway:

227



229



231

232 However, as stated above, we did not observe variations in the CO or CO₂ concentrations in our
233 experimental conditions. For the second reaction, where an alkane is formed, we compare the *n*-
234 butane, *n*-pentane and *n*-hexane infrared spectra with the residual product spectra of the ozonolysis
235 of (*E*)-2-heptenal, (*E*)-2-octenal and (*E*)-2-nonenal, respectively. The C-H stretching region from
236 -CH₂- and -CH₃ groups (2800-3032 cm⁻¹) of the alkanes was no observed in the residual product
237 spectra of the studied reactions.

238 Paulson et al.⁴⁰ have determined an OH yield of 16 % for the ozonolysis of methyl vinyl ketone
239 ($\text{CH}_2=\text{CHC}(=\text{O})\text{CH}_3$) and Uchida et al.²⁷ have reported an OH formation yields of 32 % for the
240 ozonolysis of (*Z*)-3-hexenal ($\text{CH}_3\text{CH}_2\text{CH}=\text{CHCH}_2\text{C}(\text{O})\text{H}$). Since in our ozonolysis systems it would
241 appear, based on the discussion above, that only the $\text{CH}_3(\text{CH}_2)_n\text{C}\cdot\text{HOO}\cdot$ ($n = 3, 4$ or 5) Criegee
242 biradicals will be producing OH, based on the work of Uchida et al.²⁷ we estimate that OH radical
243 production is probably of the order of 15 % or less.

244 Despite the possible effect that OH radical reactions can have on the yields of the primary carbonyls
245 measured for the ozonolysis of the C7-C9 2-alkenals, the measured yields are very similar to those
246 reported in the literature for shorter chain 2-alkenals. Grosjean et al.²⁶ have studied the product
247 formation from the ozonolysis of the C6 2-alkenal *trans*-2-hexenal and obtained formation yields
248 for the primary products glyoxal and butanal of (55.9 ± 3.7) % and (52.7 ± 5.5) %, respectively. The
249 experiments were carried out in a Teflon chamber at 298K and 760 Torr monitoring the O_3
250 concentration by ultraviolet photometry and analyzing the carbonyl compounds by liquid
251 chromatography with UV detection. In the experiments cyclohexane was added to scavenge any OH
252 radicals formed. Uchida et al.²⁷ have studied the product formation from the ozonolysis of the C6 3-
253 alkenal (*Z*)-3-hexenal in a chamber at 298 K and 1 atm using in-situ long-path Fourier transform
254 infrared (FTIR) spectroscopy for the analysis. The authors report a yield of (35 ± 1) % for the
255 primary product propanal obtained using 1,3,5-trimethylbenzene and CO as OH radical scavengers.

256 Grosjean and Grosjean²⁴ have studied the products formed in the ozonolysis of the C3 2-alkenal
257 acrolein ($\text{CH}_2=\text{CHCHO}$) and Grosjean and Grosjean²⁵ those formed in the ozonolysis of the C4
258 alkenal crotonaldehyde ($\text{CH}_3\text{CH}=\text{CHCHO}$). The experiments of Grosjean and Grosjean²⁴ on the
259 ozonolysis of acrolein were performed at 17, 14, 13 and 12°C in a 3.5 m³ Teflon chamber,
260 cyclohexane was used as an OH radical scavenger and the carbonyl products were sampled on
261 cartridges coated with 2,4-dinitrophenylhydrazine and subsequently analyzed by liquid
262 chromatography with ultraviolet detection. The main carbonyl compounds detected were
263 formaldehyde and glyoxal. The authors give amount of the carbonyls formed in ppb, however,
264 unfortunately they do not provide any yield information. The experiments of Grosjean and
265 Grosjean²⁵ on the ozonolysis of crotonaldehyde were similarly performed in a large volume FEP
266 Teflon chamber at ambient temperature and atmospheric pressure in the presence of cyclohexane as
267 an OH radical scavenger. The O_3 concentration was monitored by ultraviolet photometry and the
268 concentration of the carbonyl compounds were analyzed by liquid chromatography with UV
269 detection after collection on cartridges. In this study the authors report formation yields of the
270 primary carbonyl products glyoxal and acetaldehyde of (47 ± 2) % and (42 ± 3) %, respectively.

271 Based on the generally accepted mechanism for the ozonolysis of alkenes the sum of the yields of
272 the two primary carbonyl products formed from the two possible primary ozonide decomposition
273 channel (see Figure 4) should be unity. The sum of the primary carbonyls is (83 ± 7) % for the
274 ozonolysis of (*E*)-2-heptenal, (80 ± 6) % for the ozonolysis of (*E*)-2-octenal, (91 ± 6) % for the
275 ozonolysis of (*E*)-2-nonenal. The sums of the yields of the primary carbonyls from the ozonolysis of
276 the (*E*)-2-alkenals studied here is $\geq 80\%$ and there is no apparent preference for one of the two
277 decomposition routes of the primary ozonide with only a slight bias in the case of (*E*)-2-heptenal
278 for the glyoxal forming channel. However, it should be noted that the sum of the yields of two
279 primary carbonyl products (glyoxal and alkanal) could be higher than unity due to glyoxal
280 yield include the oxygen ejection pathway contribution. As can be deduced from the above
281 discussion on other literature studies on the ozonolysis of 2-alkenals similar yields and no trend
282 toward a particular primary ozonide decomposition channel have also been observed in these
283 studies.

284 It is interesting to note that the biradicals formed from the decomposition of the primary ozonide
285 through channels A and B (see Figure 4) are both mono-substituted biradicals, the only difference
286 being the type of the substituent. The biradical formed through channel A has an alkyl chain
287 substituent and the biradical formed through channel B has an acyl group substituent. Studies have
288 shown that the ozonolysis of asymmetrically alkyl-substituted alkenes generally results in
289 preferential formation of the more substituted biradical.^{41,42} Moreover, Wegener et al.⁴³ state that
290 after decomposition of the primary ozonide generally electron-donating substituents remain in the
291 biradical while electron acceptor substituents will be found in the carbonyl compound. However, as
292 discussed above such a preference has not observed for the 2-alkenals studied here and also for the
293 other 2-alkenals reported in the literature all of which contain an electron-acceptor, acyl, and an
294 electron-donating, alkyl, substituent. There is conjugation between the carbonyl group and the
295 double bond in the 2-alkenals and we speculate that the addition of ozone may not form a primary
296 ozonide in the classical sense as is accepted for alkyl substituted alkenes and that the preferential
297 fragmentation patterns observed for alkyl substituted alkenes may not apply for 2-alkenals and
298 possibly also 2-alkenones.

299 After subtraction of the infrared adsorptions due to the identified compounds for each of the studied
300 reactions, the residual infrared spectra (see panel D in Figures 1, S2, and S3) show distinct
301 absorption bands in the carbonyl-stretching region ($\sim 1757 \text{ cm}^{-1}$) and the C-H stretching region from
302 $-\text{CH}_2$ and $-\text{CH}_3$ groups ($2880\text{-}3000 \text{ cm}^{-1}$). As noted previously, 2-oxoaldehyde compounds are
303 potential reaction products, formation of which can not be experimentally validated due to the lack
304 of authentic samples of the compounds. Grosjean et al.²⁶ have observed the formation of 2-

305 oxobutanal with a yield of ~7.4 % in the ozonolysis (*E*)-2-hexenal, therefore, formation of 2-
306 oxoaldehydes in our study on the ozonolysis of C7-C9 2-alkenals is expected to be likely. In order
307 to try and verify formation of 2-oxoaldehydes in the ozonolysis reactions infrared spectra have been
308 computed for 2-oxopentanal (proposed product from the reaction of (*E*)-2-heptenal + O₃), for 2-
309 oxohexanal (proposed product from the reaction of (*E*)-2-octenal + O₃) and for 2-oxoheptanal
310 (proposed product from the reaction of (*E*)-2-nonenal + O₃). The computed spectra were obtained
311 with the Gaussian 09 package at the B3LYP/6-311++G (d, 2p) level of theory.⁴⁴⁻⁴⁶ Figure 5 shows a
312 comparison between the computed IR spectrum for the expected product 2-oxopentanal and the
313 residual experimental product IR spectrum obtained from the ozonolysis (*E*)-2-heptenal after
314 subtraction of the primary carbonyl products. Figures S8 and S9 show the corresponding
315 comparisons for the ozonolysis of (*E*)-2-octenal and (*E*)-2-nonenal where 2-oxohexanal and 2-
316 oxoheptanal, respectively, are the potential 2-oxoaldehyde products. The salient features from the
317 residual spectra for each of the studied reactions show similarity with the computed spectra. This
318 similarity suggests that many of the absorption features in the residual product spectra obtained
319 from the ozonolysis of (*E*)-2-heptenal, (*E*)-2-octenal and (*E*)-2-nonenal are quite possibly due to the
320 formation of 2-oxopentanal, 2-oxohexanal and 2-oxoheptanal, respectively. However, an infrared
321 spectrum of each of the oxoaldehyde compounds obtained from an authentic sample of the
322 compound is necessary for an absolute validation of their formation. The residual spectra may also
323 contain absorptions from other carbonyl compounds, such as the hydroxydicarbonyl compounds
324 from the isomerization of the alkoxy radical that have been previously mentioned, however, in
325 Figures 1, S1 and S2 there are not observed the infrared band corresponding to the stretching of OH
326 group (3500-3600cm⁻¹), other possibility is the formation of epoxy compounds, even though the
327 epoxy pathway in gas phase ozonolysis reactions is considered to be a minor pathway.⁴⁷⁻⁴⁸
328 In summary, the ozonolysis of the C7-C9 (*E*)-2-alkenal compounds studied in this work leads to the
329 formation as primary products the dicarbonyl compound glyoxal and the corresponding saturated
330 aldehydes pentanal, hexanal and heptanal. The yields of the primary carbonyl products were all
331 quite similar with combined total carbonyl yields of ≥ 80% for each of the studied reactions. No
332 preference was found for the two possible primary ozonide decomposition in agreement with other
333 studies on shorter chain 2-alkenals and contrary to what one would expect based ozonolysis studies
334 of alkyl substituted alkenes.

335
336
337
338

339 **Atmospheric implications**

340

341 In a previous work, we have reported the atmospheric lifetimes of the studied 2-alkenals using the
342 typical ambient concentrations for the tropospheric oxidants (OH, O₃, Cl). The calculated lifetimes
343 indicated that the reaction with OH and NO₃ (few hours) radicals are the main degradation
344 processes for these aldehydes in the atmosphere, reaction with O₃ possibly being of some
345 importance in regions with high levels of O₃.¹⁷ The ozonolysis reactions of these unsaturated
346 aldehydes have been in this study and some other studies to be sources for alkyl aldehydes,
347 dialdehydes and possibly other oxygenated compounds. Glyoxal can be degraded in the atmosphere
348 by reaction with OH radicals⁴⁹ and via photolysis.⁵⁰ Fu et al.⁵¹ have estimated the global production
349 budget of glyoxal to be ~45 Tg/annum, even though, isoprene oxidation contributes to 47% of this
350 globally glyoxal budget. Moreover, glyoxal plays an important role in global SOA formation via
351 irreversible uptake by aqueous aerosols and clouds,⁵¹⁻⁵⁵ for example, De Haan et al.⁵⁵ have estimated
352 that glyoxal can produce 1 Tg C/year SOA due to self-reactions in a evaporating droplets.
353 Additionally, it can be removed from the atmosphere through wet deposition due to its high water
354 solubility.⁵⁶

355 The alkyl aldehydes products of the studied reactions also have as main degradation processes in
356 the atmosphere the reaction with OH radicals and photolysis. For example, pentanal has a lifetime
357 of 5.1 h due to the reaction with OH radical (calculated using a noon time value of [OH] = 2 × 10⁶
358 molecule cm⁻³) and a lifetime due to photolysis of 17 h.⁵⁷ The lifetime of hexanal due to the reaction
359 with OH radicals has been estimated by Jiménez et al.⁵⁸ to be 10 h using a 24 h average of [OH]=
360 1×10⁶ molecule cm⁻³ at 298 K, which reduces to 4.9 h if [OH]= 2×10⁶ molecule cm⁻³ is used in the
361 lifetime calculation. The lifetime of this aldehyde due to photolysis has been estimated to be < 48 h
362 by Jiménez et al.⁵⁸ Finally, heptanal has an estimated lifetime of 4.7 h due to reaction with OH
363 when calculated using a noon time value of [OH]= 2×10⁶ molecule cm⁻³ and k_{OH}= 2.96×10⁻¹¹
364 molecule⁻¹ cm³ s⁻¹ ¹⁸ and a photolysis lifetime of 17 h, obtained using the photolysis rate of (1.65 ±
365 0.03)×10⁻⁵ s⁻¹ from Paulson et al.⁵⁹ These C5-C7 alkyl aldehydes have been detected in urban, rural
366 and forest environments.⁶⁰⁻⁶³ The atmospheric degradation of pentanal, hexanal, heptanal and
367 glyoxal can produce free radical species that can contribute to O₃ formation and in the presence of
368 NO_x could form organic nitrates or peroxy nitrates which transport NO_x species to remote
369 environments.

370

371

372

373 **Acknowledgments**

374

375 We gratefully acknowledge the financial support for this research provided by the EU project
376 EUROCHAMP2 (E2-2013-02-27-0086), CONICET, PIP- GI 2010-2012-cod: 11220090100623
377 (Argentina), SECyT-UNC 14306/24. (Argentina) and FONCyT Préstamo BID 1201/OC-AR
378 (Argentina). E. Gaona Colmán wishes to thank CONICET for a PhD fellowship. M. B. Blanco
379 wishes to acknowledge the Alexander von Humboldt Foundation (Germany) for support.

380

381 **References**

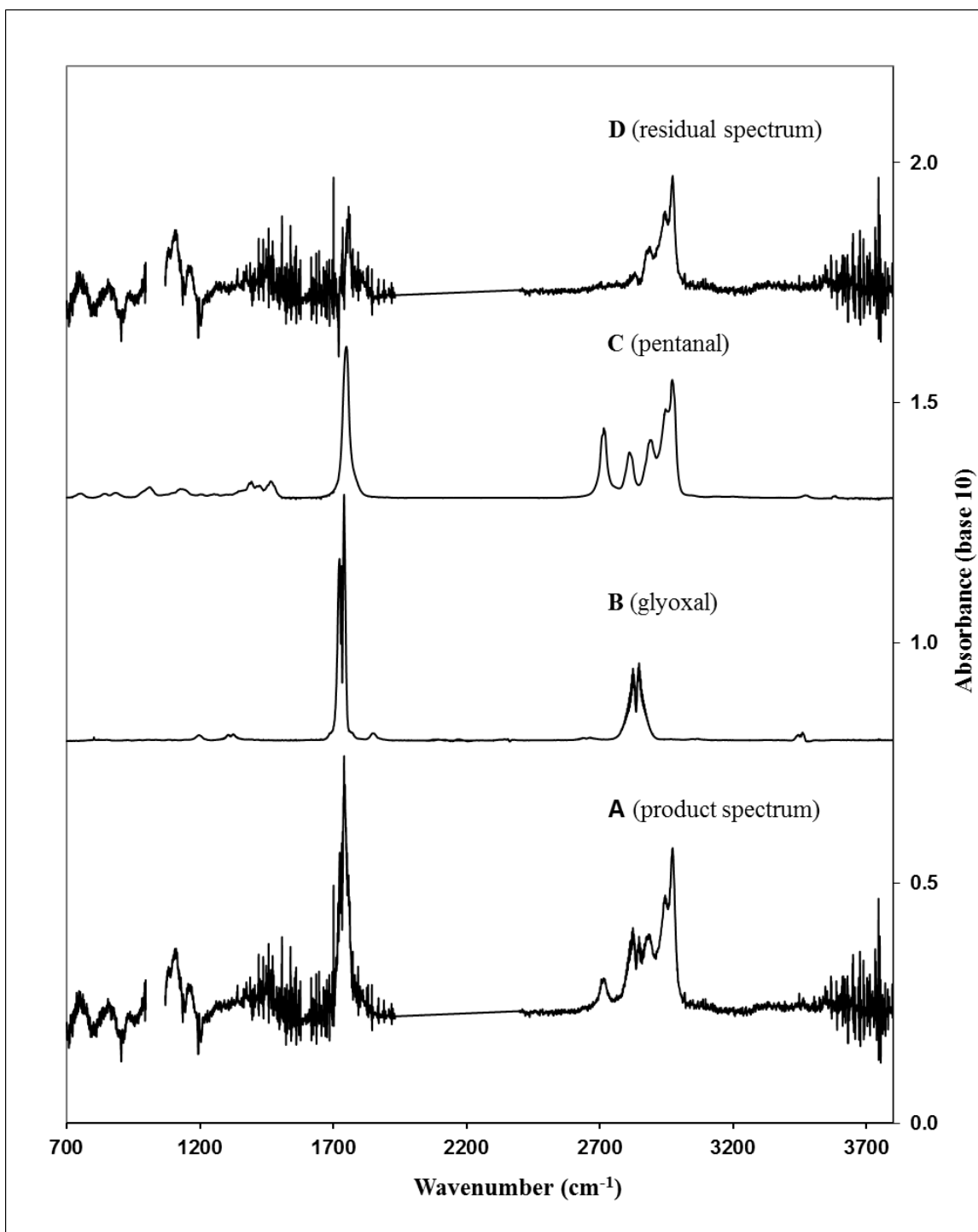
382

- 383 (1) Anjou, K.; von Sydow, E. The Aroma of Cranberries I. *Vaccinium vitis-idaea* L. *Acta Chem.*
384 *Scand.* **1967**, 21, 945-952.
- 385 (2) Zhu, J. C.; Chen, F.; Wang, L. Y.; Niu, Y. W.; Chen, H. X.; Wang, H. L.; Xiao, Z. B.
386 Characterization of the Key Aroma Volatile Compounds in Cranberry (*Vaccinium macrocarpon*
387 Ait.) Using Gas Chromatography–Olfactometry (GC-O) and Odor Activity Value (OAV). *J.*
388 *Agric. Food Chem.* **2016**, 64, 4990– 4999.
- 389 (3) Beaulieu, J. C.; Lea, J. M. Characterization and Semiquantitative Analysis of Volatiles in
390 Seedless Watermelon Varieties Using Solid-Phase Microextraction. *J. Agric. Food Chem.* **2006**,
391 54, 7789–7793
- 392 (4) Petersen, M. A.; Poll, L.; Larsen, L. M. Comparison of Volatiles in Raw and Boiled Potatoes
393 Using a Mild Extraction Technique Combined with GC Odour Profiling and GC-MS. *Food*
394 *Che.* **1998**, 61, 4,461-466.
- 395 (5) Palma-Harris, C.; McFeeters, R. F.; Fleming, H. Solid-Phase Microextraction (SPME)
396 Technique for Measurement of Generation of Fresh Cucumber Flavor Compounds. *J. Agric.*
397 *Food Chem.* **2001**, 49, 4203–4207.
- 398 (6) Atiama-Nurbel, T.; Quilici, S.; Boyer, E., Deguine, J.-P.; Glenac, S.; Bialecki, A. Volatile
399 Constituents of *Cucumis sativus*: Differences Between Five Tropical Cultivars. *Chem. Nat.*
400 *Compd.* **2015**, 51, 4, 771-775
- 401 (7) Fuhrmann, E.; Grosch, W. Character Impact Odorants of the Apple Cultivars Elstar and Cox
402 Orange. *Nahrung/Food.* **2002**, 46, 3, 187-193.
- 403 (8) Zhou, A.; McFeeters, R. F.; Fleming, H. P. Development of Oxidized Odor and Volatile
404 Aldehydes in Fermented Cucumber Tissue Exposed to Oxygen. *J. Agric. Food Chem.* **2000**, 48,
405 193–197.
- 406 (9) Xu, Y.; Barringer, S. E. Effect of Temperature on Lipid-Related Volatile Production in Tomato
407 Puree. *J. Agric. Food Chem.* **2009**, 57, 9108–9113.
- 408 (10) Zhu, X.; Tang, X.; Anderson, V. E.; Sayre, L. M. Mass Spectrometric Characterization of
409 Protein Modification by the Products of Nonenzymatic Oxidation of Linoleic Acid. *Chem. Res.*
410 *Toxicol.* **2009**, 22, 1386–1397.
- 411 (11) Cahill, T. M.; Okamoto, R. Emissions of Acrolein and Other Aldehydes from Biodiesel-
412 Fueled Heavy-Duty Vehicles. *Environ. Sci. Technol.* **2012**, 46, 8382– 8388.
- 413 (12) do N. Batista, L.; Da Silva, V. F.; Pissurno, E. C. G.; da Conceicao Soares, T.; de Jesus, M.
414 R.; Kunigami, C. N.; Brasil, M. G.; da Fonseca, M. G. Formation of Toxic Hexanal,
415 2-Heptenal and 2,4-Decadienal During Biodiesel Storage and Oxidation. *Environ. Chem. Lett.*
416 **2015**, 13, 353–358
- 417 (13) Guillén, M. D.; Uriarte, P. S. Aldehydes Contained in Edible Oils of a Very Different Nature
418 After Prolonged Heating at Frying Temperature: Presence of Toxic Oxygenated

- 419 α , β - Unsaturated Aldehydes. *Food Chem.* **2012**, 131, 915–926.
- 420 (14) Shalamzari, M. S.; Kahnt, A.; Vermeylen, R.; Kleindienst, T. E.; Lewandowski, M.;
421 Cuyckens, F.; Maenhaut, W.; Claeys, M. Characterization of Polar Organosulfates in
422 Secondary Organic Aerosol from the Green Leaf Volatile 3-Z-Hexenal. *Environ. Sci.*
423 *Technol.* **2014**, 48, 12671-12678.
- 424 (15) Shalamzari, M. S.; Vermeylen, R.; Blockhuys, F.; Kleindienst, T. E.; Lewandowski, M.;
425 Szmigielski, R.; Rudzinski, K.J.; Spólnik, G.; Danikiewicz, W.; Maenhaut, W.; Claeys, M.
426 Characterization of Polar Organosulfates in Secondary Organic Aerosol from the Unsaturated
427 Aldehydes 2-E-Pentenal, 2-E-Hexenal, and 3-Z-Hexenal. *Atmos. Chem. Phys.* **2016**, 16,
428 7135-7148.
- 429 (16) Richards-Henderson, N. K.; Hansel, A. k.; Valsaraj, K. T.; Anastasio, C. Aqueous Oxidation
430 of Green Leaf Volatiles by Hydroxyl Radical as a Source of SOA: Kinetics and SOA Yields.
431 *Atmos. Environ.* **2014**, 95, 105-112.
- 432 (17) Gaona Colmán, E.; Blanco, M. B.; Barnes, I.; Teruel, M. A. Ozonolysis of a Series of C7–C9
433 Unsaturated Biogenic Aldehydes: Reactivity Study at Atmospheric Pressure. *RSC Adv.* **2015**,
434 5, 30500-30506.
- 435 (18) Albaladejo, J.; Ballesteros, B.; Jiménez, E.; Martín, P.; Martínez, E. A PLP–LIF Kinetic Study
436 of the Atmospheric Reactivity of a Series of C4–C7 Saturated and Unsaturated Aliphatic
437 Aldehydes with OH. *Atmos. Environ.* **2002**, 36, 3231-3239.
- 438 (19) Davis, M. E.; Gilles, M. K.; Ravishankara, A. R.; Burkholder, J. B. Rate Coefficients for the
439 Reaction of OH with (E)-2-Pentenal, (E)-2-Hexenal, and (E)-2-Heptenal. *Phys. Chem. Chem.*
440 *Phys.* **2007**, 9 2240 – 2248.
- 441 (20) Gao, T.; Andino, J. M.; Rivera, C. C.; Márquez, M. F. Rate Constants of the Gas-Phase
442 Reactions of OH Radicals with trans-2-Hexenal, trans-2-Octenal, and trans-2-Nonenal. *Int. J.*
443 *Chem. Kinet.* **2009**, 41, 483–489.
- 444 (21) Zhao, Z.; Husainy, S.; Smith, G. D. Kinetics Studies of the Gas-Phase Reactions of NO₃
445 Radicals with Series of 1-Alkenes, Dienes, Cycloalkenes, Alkenols, and Alkenals. *J. Phys.*
446 *Chem. A.* **2011**, 115, 44, 12161–12172.
- 447 (22) Kerdouci, J.; Picquet-Varrault, B.; Durand-Jolibois, R.; Gaimoz, C.; Doussin, J. F. An
448 Experimental Study of the Gas-Phase Reactions of NO₃ Radicals with a Series of Unsaturated
449 Aldehydes: trans-2-Hexenal, trans-2-Heptenal, and trans-2-Octenal. *J. Phys. Chem. A.* **2012**,
450 116, 41, 10135-10142.
- 451 (23) Rodríguez, D.; Rodríguez, A.; Notario, A.; Aranda, A.; Díaz-de-Mera, Y.; Martínez, E.
452 Kinetic Study of the Gas-Phase Reaction of Atomic Chlorine with a Series of Aldehydes.
453 *Atmos. Chem. Phys.* **2005**, 5, 3433-3440.
- 454 (24) Grosjean, E.; Williams II, E. L.; Grosjean, D. Atmospheric Chemistry of Acrolein. *Sci. Total*
455 *Environ.* **1994**, 153, 195-202.
- 456 (25) Grosjean, E.; Grosjean, D. The Gas Phase Reaction of Unsaturated Oxygenates with Ozone:
457 Carbonyl Products and Comparison with the Alkene-Ozone Reaction. *J. Atmos. Chem.* **1997**,
458 27, 271–289.
- 459 (26) Grosjean, E.; Grosjean, D.; Seinfeld, J. H. Gas-Phase Reaction of Ozone with trans-2-Hexenal,
460 trans-2-Hexenyl Acetate, Ethylvinyl Ketone, and 6-Methyl-5-hepten-2-one. *Int. J. Chem.*
461 *Kinet.* **1996**, 28, 373-382.
- 462 (27) Uchida, R.; Sato, K.; Imamura, T. Gas-Phase Ozone Reactions with Z-3-Hexenal and Z-3-
463 Hexenol: Formation Yields of OH Radical, Propanal, and Ethane. *Chem. Lett.* **2015**, 44, 457-
464 458.
- 465 (28) Barnes, I; Becker, K. H.; Zhou, T. Near UV Absorption Spectra and Photolysis Products of
466 Difunctional Organic Nitrates. *J. Atmos. Chem.* **1993**, 17, 353-373.
- 467 (29) Barnes, I.; Becker, K. H.; Mihalopoulos, N. An FTIR Product Study of the Photooxidation of
468 Dimehtyl Disulfide. *J. Atmos. Chem.* **1994**, 18, 267-289.
- 469 (30) Volkamer R; Spietz P; Burrows J.; Platt U. High-Resolution Absorption Cross-Section of

- 470 Glyoxal in the UV/Vis and IR Spectral Ranges. *J. Photochem. Photobiol. A Chem.* **2005**, 172,
471 35-46.
- 472 (31) Beaver, M. R.; Elrod, M. J.; Garland, R. M.; Tolbert, M. A. Ice Nucleation in Sulfuric
473 Acid/Organic Aerosols: Implications for Cirrus Cloud Formation. *Atmos. Chem. Phys.* **2006**, 6,
474 3231–3242
- 475 (32) Atkinson, R.; Carter, W.P.L. Kinetics and Mechanisms of the Gas-Phase Reactions of
476 Ozone with Organic Compounds under Atmospheric Conditions. *Chem. Rev.* **1984**, 84, 437-
477 470.
- 478 (33) Horie, O.; Moortgat, G. K. Gas-Phase Ozonolysis of Alkenes. Recent Advances in Mechanistic
479 Investigations. *Acc. Chem. Res.* **1998**, 31, 387-396.
- 480 (34) Atkinson, R. Gas-Phase Tropospheric Chemistry of Volatile Organic Compounds: 1. Alkanes
481 and Alkenes. *J. Phys. Chem. Ref. Data.* **1997**, 26, 215-290.
- 482 (35) Calvert, J. G.; Atkinson, R.; Kerr, J. A.; Madronich, Moorgat, G. K.; Wallington, T. J.;
483 Yarwood, G. *The Mechanisms of Atmospheric Oxidation of Alkenes*. Oxford University Press,
484 Oxford. **2000**.
- 485 (36) Calvert, J. G.; Orlando, J. J.; Stockwell, W. R.; Wallington, T. J. *The Mechanisms of Reactions*
486 *Influencing Atmospheric Ozone*. Oxford University Press, Oxford. **2015**.
- 487 (37) Rickard, A. R.; Johnson, D.; McGill, C. D.; Marston, G. OH Yields in the Gas-Phase Reactions
488 of Ozone with Alkenes. *J. Phys. Chem. A* 1999, 103, 7656-7664.
- 489 (38) Dixon, A. R.; Xue, T.; Sanov, A. Spectroscopy of Ethylenedione. *Angew. Int. Ed.* **2015**, 54,
490 8764-8767.
- 491 (39) Miller, F. A.; Fateley, W. G. The Infrared Spectrum of Carbon Suboxide. *Spectrochim. Acta.*
492 1964, 20, 253-266.
- 493 (40) Paulson, S. E.; Chung, M.; Sen, A. D.; Orzechowska, G. Measurement of OH Radical
494 Formation from the Reaction of Ozone with Several Biogenic Alkenes. *J. Geophys. Res.* **1998**,
495 103, D19, 25,533-25,539.
- 496 (41) Grosjean, E.; Grosjean, D. Carbonyl Products of the Gas-Phase Reaction of Ozone with 1-
497 Alkenes. *Atmos. Environ.* **1996**, 30, 24, 4107-4113.
- 498 (42) Tuazon, E. C.; Aschmann, S. M.; Arey, J.; Atkinson, R. Products of the Gas-Phase Reactions
499 Of O₃ with a Series of Methyl-Substituted Ethenes. *Environ. Sci. Technol.* **1997**, 31, 3004-
500 3009.
- 501 (43) Wegener, R.; Brauers, T.; Koppmann, R.; Rodríguez Bares, S.; Rohrer, F.; Tillmann, R.;
502 Wahner, A.; Hansel, A.; Wisthaler, A. Simulation Chamber Investigation of the Reactions of
503 Ozone with Short-Chained Alkenes. *J. Geophys. Res.* **2007**, 112, D13301.
- 504 (44) Becke, A. D. Density-Functional Thermochemistry. III. The Role of Exact Exchange. *J. Chem.*
505 *Phys.* **1993**, 98, 5648 – 5652.
- 506 (45) Lee, C.; Yang, W.; Parr, R. G. Development of the Colle-Salvetti Correlation-Energy Formula
507 into a Functional of the Electron Density. *Phys. Rev. B.* **1988**, 37, 785 – 789.
- 508 (46) Miehlich, B.; Savin, A.; Stoll, H.; Preuss, H. Results Obtained with the Correlation Energy
509 Density Functionals of Becke and Lee, Yang and Parr. *Chem. Phys. Lett.* **1989**, 157, 200 –206.
- 510 (47) Atkinson, R. and Arey, J. Gas-phase tropospheric chemistry of biogenic volatile organic
511 compounds: a review. *Atmos. Environ.* **2003**, 37, S197-S219.
- 512 (48) Kramp, F. and Paulson, S. E. The gas phase reaction of ozone with 1,3-butadiene: formation
513 yields of some toxic products. *Atmos. Environ.* **2000**, 34, 35-43.
- 514 (49) Plum, C. N.; Sanhueza, E.; Atkinson, R.; Carter, W. P. L.; Pitts, J. N. Jr. OH Radical Rate
515 Constants and Photolysis Rates of α -Dicarbonyls. *Environ. Sci. Technol.* **1983**, 17, 479-484.
- 516 (50) Tadić, J.; Moortgat, G. K.; Wirtz, K. Photolysis of Glyoxal in Air. *J. Photochem. Photobiol., A.*
517 **2006**, 177, 116-124.
- 518 (51) Fu, T. M.; Jacob, D. J.; Wittrock, F.; Burrows, J. P.; Vrekoussis, M.; Henze, D. K. Global
519 Budgets of Atmospheric Glyoxal and Methylglyoxal, and Implications for Formation of
520 Secondary Organic Aerosols. *J. Geophys. Res.* **2008**, 113, D15303.

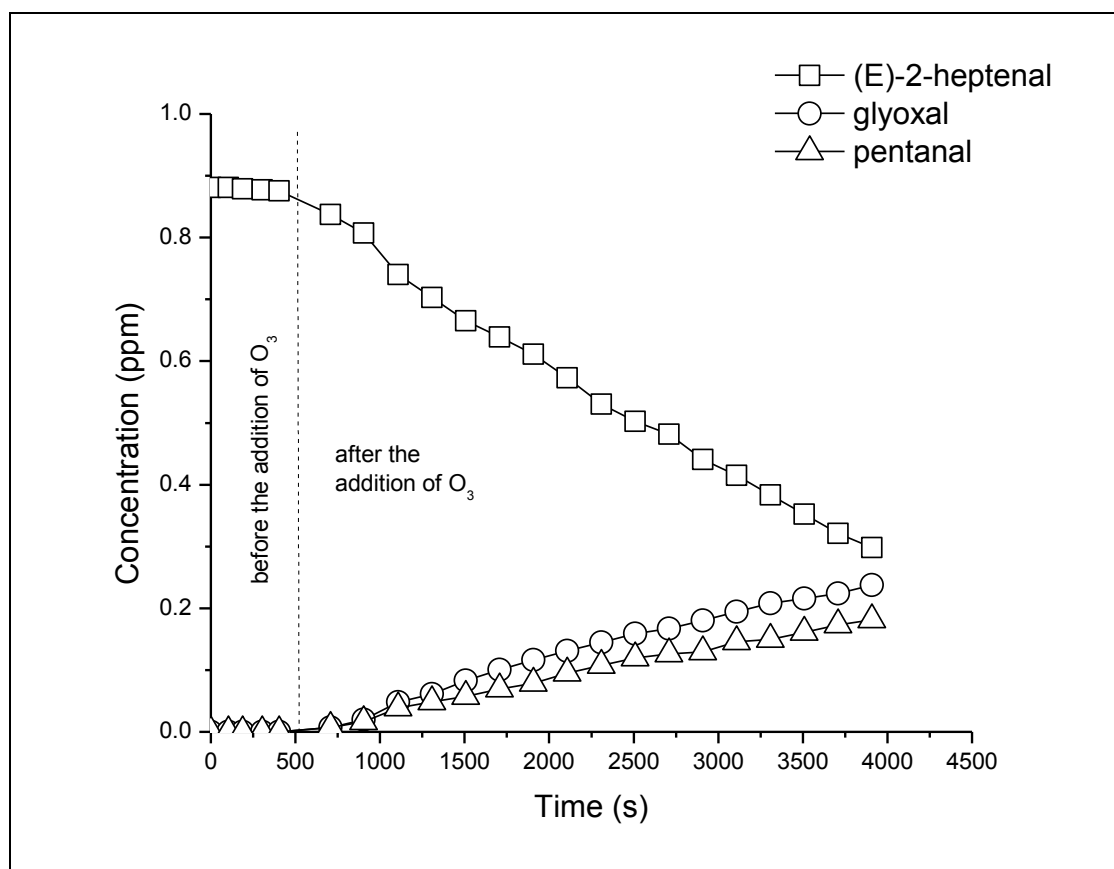
- 521 (52) Hastings, W. P.; Koehler, C. A.; Bailey, E. L.; De Haan, D. O. Secondary Organic Aerosol
522 Formation by Glyoxal Hydration and Oligomer Formation: Humidity Effects and Equilibrium
523 Shifts During Analysis. *Environ. Sci. Technol.* **2005**, 39, 8728–873.
- 524 (53) Liggio, J.; Li, S. M.; McLaren, R. Reactive Uptake of Glyoxal by Particulate Matter. *J.*
525 *Geophys. Res.* **2005**, 110, D10304.
- 526 (54) Schaefer, T.; van Pinxteren, D.; Herrmann, H. Multiphase Chemistry of Glyoxal: Revised
527 Kinetics of the Alkyl Radical Reaction with Molecular Oxygen and the Reaction of Glyoxal
528 with OH, NO₃, and SO₄⁻ in Aqueous Solution. *Environ. Sci. Technol.* **2015**, 49, 343-350.
- 529 (55) De Haan, D. O.; Corrigan, A. L.; Tolbert, M. A.; Jimenez, J. L.; Wood, S. E.; Turley, J. J.
530 Secondary Organic Aerosol Formation by Self-Reactions of Methylglyoxal and Glyoxal in
531 Evaporating Droplets. *Environ. Sci. Technol.* **2009**, 43, 8184–8190.
- 532 (56) Matsunaga, S. N.; Guenther, A.; Izawa, Y.; Wiedinmyer, C.; Greenberg, J.; Kawamura, K.
533 Importance of Wet Precipitation as a Removal and Transport Process for Atmospheric Water
534 Soluble Carbonyls. *Atmos. Environ.* **2007**, 41, 790-796.
- 535 (57) Tadić, J.; Juranić, I.; Moortgat, G. K. Pressure Dependence of Photooxidation of Selected
536 Carbonyl Compounds in Air: n-Butanal and n-Pentanal. *J. Photochem. Photobiol., A.* **2001**,
537 143, 169-179.
- 538 (58) Jiménez, E.; Lanza, B.; Martínez, E.; Albaladejo, J. Daytime Tropospheric Loss of Hexanal
539 and trans-2-Hexenal: OH Kinetics and UV Photolysis. *Atmos. Chem. Phys.* **2007**, 7, 1565–
540 1574.
- 541 (59) Paulson, S. E.; Liu, D. L.; Orzechowska, G. E. Photolysis of Heptanal. *J. Org. Chem.* **2006**,
542 71, 6403 -6408.
- 543 (60) Ciccioli, P.; Brabcaleoni, E.; Frattoni, M.; Cecinato, A.; Brachetti, A. Ubiquitous Occurrence
544 of Semi-Volatile Carbonyl Compounds in Tropospheric Samples and their Possible Sources.
545 *Atmos. Environ.* **1993**, 27A, 12, 1891-1901
- 546 (61) Grosjean, E.; Grosjean, D.; Fraser, M. P.; Cass, G. R. Air Quality Model Evaluation Data for
547 Organics. 2. C1-C14 Carbonyls in Los Angeles Air. *Environ. Sci. Technol.* **1996**, 30, 2687-
548 2703
- 549 (62) Hurst Bowman, J.; Barket, Jr. D.; Shepson, P. B. Atmospheric Chemistry of Nonanal. *Environ.*
550 *Sci. Technol.* **2003**, 37, 2218-2225
- 551 (63) Guo, S.; Chen, M.; Tan, J. Seasonal and Diurnal Characteristics of Atmospheric Carbonyls in
552 Nanning, China. *Atmos. Res.* **2016**, 169, 46–53
- 553
- 554



555

556 **Figure 1:** Panel A shows the infrared spectrum of a (*E*)-2-heptenal/ O_3 /air gas mixture after reaction
 557 and subtraction of residual (*E*)-2-heptenal. Panels B and C show reference spectra of glyoxal and
 558 pentanal, respectively. Panel D shows the residual product spectrum obtained after subtraction of
 559 features due to the reference spectra from the spectrum in panel A. (A straight line is presented
 560 between 1900-2400 cm^{-1} for the spectra in panel A and D avoiding the CO_2 and CO absorption)

561



563

564 **Figure 2:** Concentration-time profiles of (*E*)-2-heptenal and the reaction products glyoxal and
565 pentanal obtained from a (*E*)-2-heptenal / O_3 /air reaction mixture.

566

567

568

569

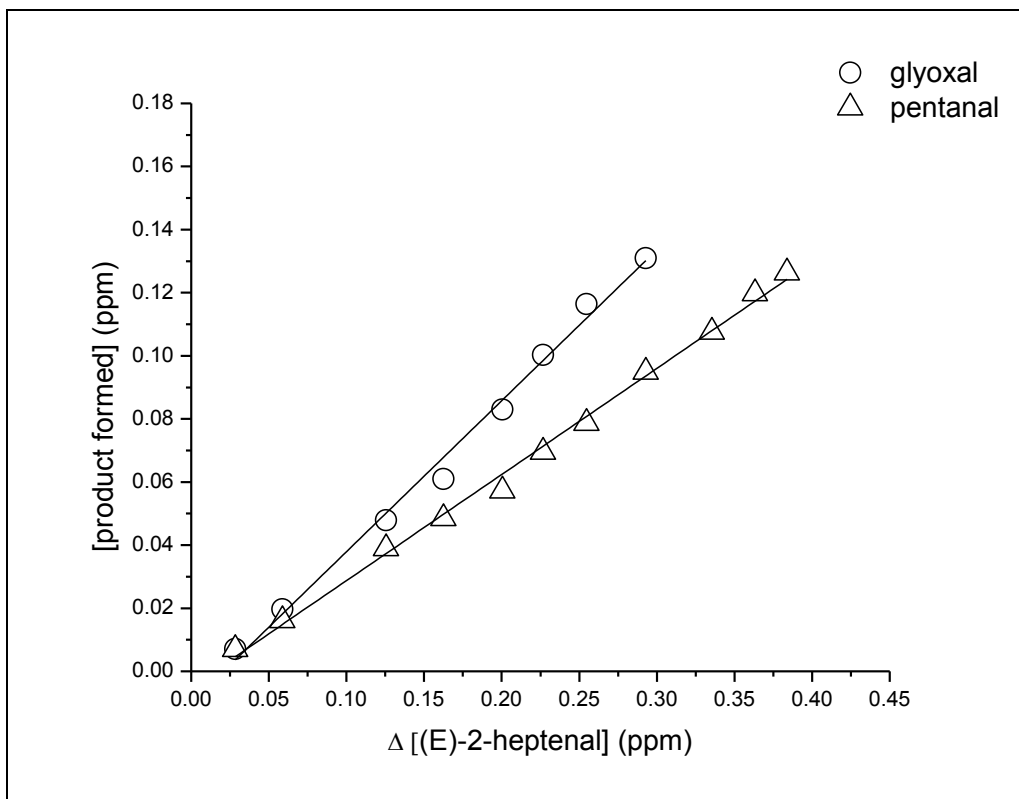
570

571

572

573

574



575

576 **Figure 3:** Plots of the concentrations of the reaction products glyoxal and pentanal as a function of
 577 reacted (*E*)-2-heptenal obtained from experiments performed on (*E*)-2-heptenal /O₃/air reaction
 578 mixtures.

579

580

581

582

583

584

585

586

587

588

589

590

591

592

593

594

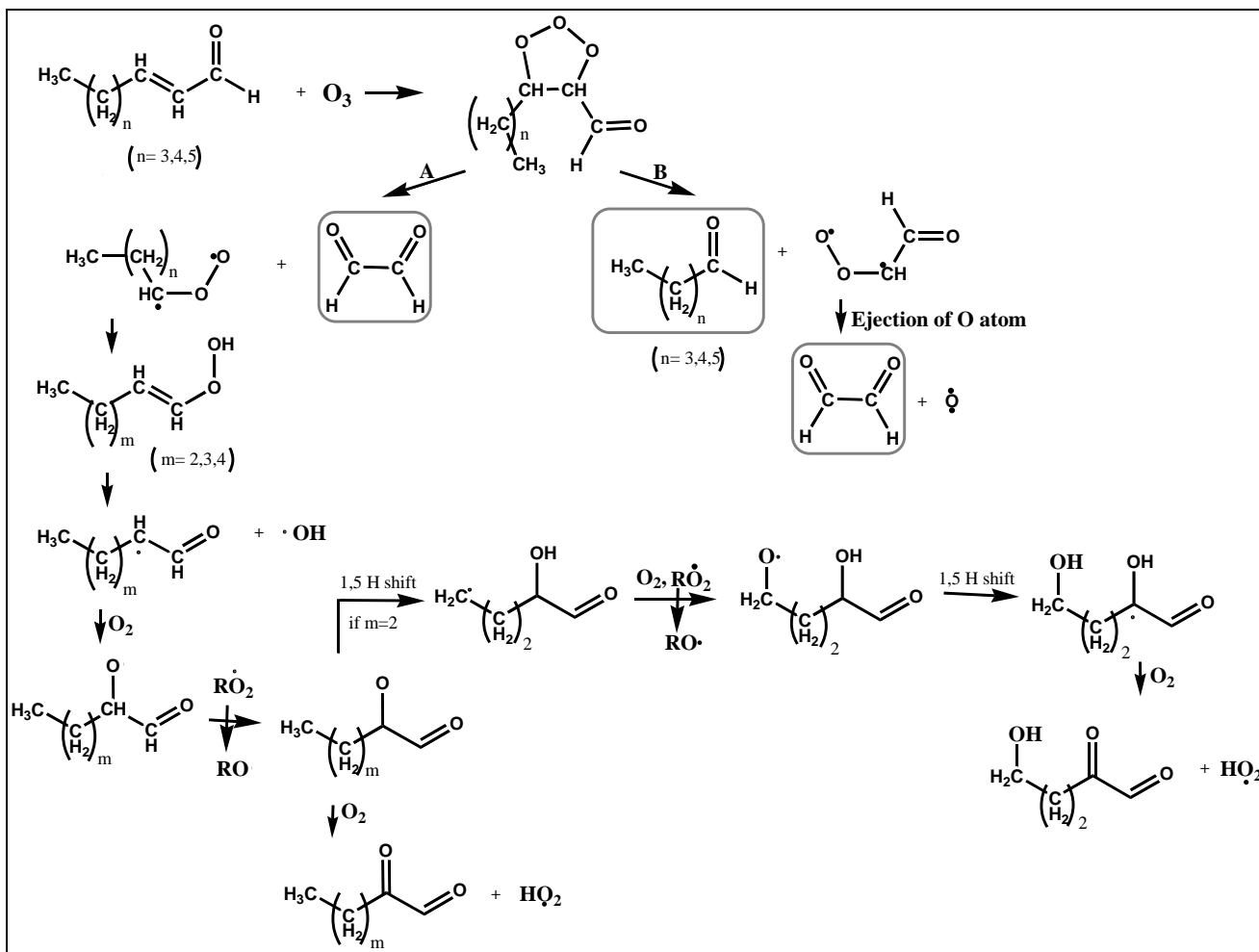
595 **Table 1**

596 Formation yields of the oxidation products identified in the ozonolysis of (*E*)-2-heptenal, (*E*)-2-
 597 octenal and (*E*)-2-nonenal at 298K in 750 ± 10 Torr of air.

Compound	Product	Yield (%)
<i>(E)</i> -2-heptenal	HC(O)C(O)H	50 ± 4
	Glyoxal	48 ± 4
		average: 49 ± 4
	CH ₃ (CH ₂) ₃ C(O)H	
	Pentanal	35 ± 3
		33 ± 2
	average: 34 ± 3	
<i>(E)</i> -2-octenal	HC(O)C(O)H	41 ± 3
	Glyoxal	41 ± 3
		average: 41 ± 3
	CH ₃ (CH ₂) ₄ C(O)H	
	Hexanal	38 ± 2
		39 ± 3
	average: 39 ± 3	
<i>(E)</i> -2-nonenal	HC(O)C(O)H	45 ± 3
	Glyoxal	44 ± 3
		average: 45 ± 3
	CH ₃ (CH ₂) ₅ C(O)H	
	Heptanal	47 ± 2
		45 ± 3
	average: 46 ± 3	

598

599



600
601

602 **Figure 4:** Simplified mechanism for the reaction of O₃ with (*E*)-2-heptenal, (*E*)-2-octenal and (*E*)-
603 2-nonenal.

604

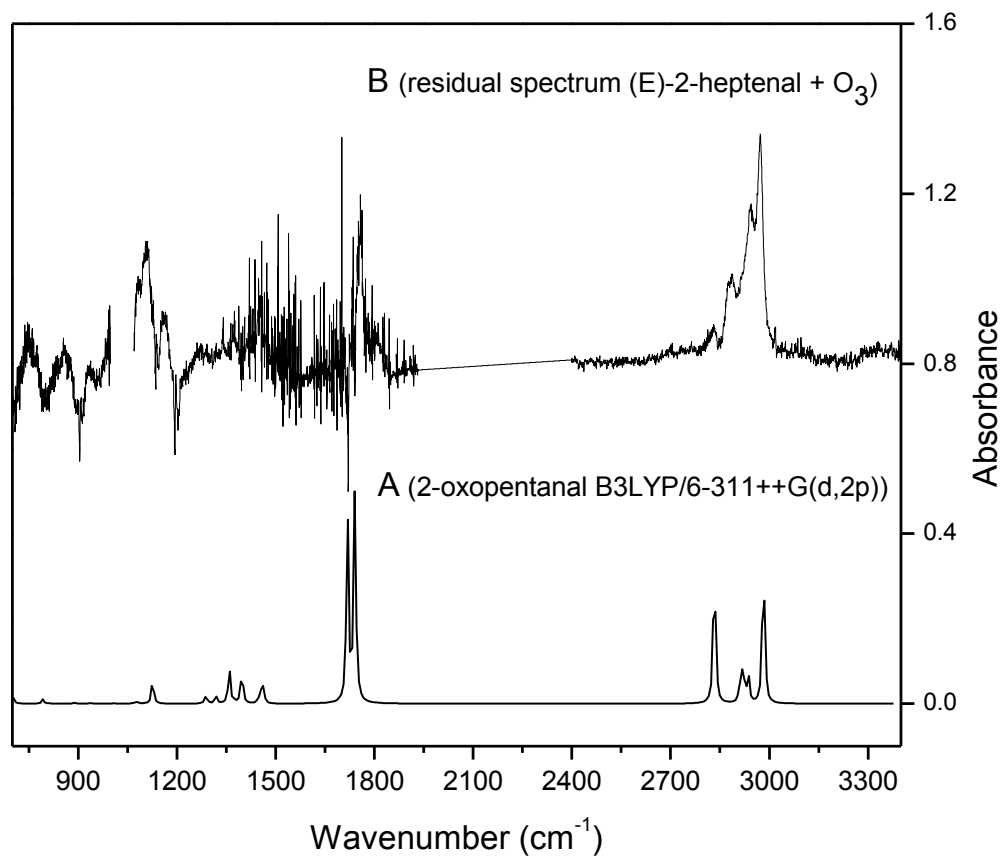
605

606

607

608

609



610 **Figure 5:** Comparison of a computed IR spectrum for the expected product 2-oxopentanal (A) with
 611 the residual product IR spectrum (B) obtained from an experiment with a (*E*)-2-heptenal/O₃/air
 612 mixture. (A straight line is presented between 1900-2400 cm⁻¹ for the residual product spectrum
 613 avoiding the CO₂ and CO absorption)
 614

615

616

617

618

619